

## Gravitational Radiation from a Naked Singularity. II

— Even-Parity Perturbation —

Hideo Iguchi <sup>\*</sup>, Tomohiro Harada <sup>†</sup>  
*Department of Physics, Kyoto University,  
Kyoto 606-8502, Japan*

and

Ken-ichi Nakao <sup>‡</sup>  
*Department of Physics, Osaka City University,  
Osaka 558-8585, Japan*

A naked singularity occurs in the generic collapse of an inhomogeneous dust ball. We study the even-parity mode of gravitational waves from a naked singularity of the Lemaître-Tolman-Bondi spacetime. The wave equations for gravitational waves are solved by numerical integration using the single null coordinate. The result implies that the metric perturbation grows when it approaches the Cauchy horizon and diverges there, although the naked singularity is not a strong source of even-parity gravitational radiation. Therefore, the Cauchy horizon in this spacetime should be unstable with respect to linear even-parity perturbations.

### I. INTRODUCTION

The singularity theorems reveal that the occurrence of singularities is a generic property of spacetime in general relativity [1–3]. However, these theorems state nothing about the detailed features of the singularities themselves; for example, we do not get information from these theorems about whether or not the predicted singularity is naked. Here, “naked” means that the singularity is in principle observable. A singularity is a boundary of spacetime. Hence, in order to obtain a solution of hyperbolic field equations for matter, gauge fields and spacetime itself in the causal future of a naked singularity, we need to impose a boundary condition on it. However, we do not yet know physically reasonable boundary conditions for singularities, and hence to avoid this difficulty, the cosmic censorship hypotheses (CCH) proposed by Penrose [4,5] are often adopted in the analysis of physical phenomena involving strong gravitational fields.

Unfortunately no one has ever succeeded in the proof of any version of the CCH. There is no precise statement of CCH which can be readily proved at this time. Given this situation it is worth trying to obtain counterexamples. Much effort has been made to search for naked singularity formation in gravitational collapse.

In the Lemaître-Tolman-Bondi (LTB) spacetime [6,7], a naked shell-focusing singularity appears from generic initial data for spherically symmetric configurations of the rest mass density and a specific energy of the dust fluid [8–11]. The initial functions in the most general expandable form have been considered [12]. The matter content in this spacetime may satisfy even the dominant energy condition. These results are summarized as follows: In this spacetime, a naked singularity appears from generic initial data for spherically symmetric configurations of the rest mass density and a specific energy of the dust fluid. Shapiro and Teukolsky numerically studied evolution of collisionless gas spheroids with fully general relativistic simulations [13]. They found some evidence that prolate spheroids with sufficiently elongated initial configurations, and even with some angular momentum, may form naked singularities. Ori and Piran numerically examined the structure of self-similar spherical collapse solutions for a perfect fluid with a barotropic equation of state [14,15]. They showed that there is a globally naked singularity in a significant part of the space of

---

<sup>\*</sup> Electronic address: iguchi@tap.scphys.kyoto-u.ac.jp

<sup>†</sup> Electronic address: harada@tap.scphys.kyoto-u.ac.jp

<sup>‡</sup> Electronic address: knakao@sci.osaka-cu.ac.jp

self-similar solutions. Joshi and Dwivedi analytically investigated the self-similar spherically symmetric collapse of a perfect fluid with a similar equation of state [16]. Harada numerically investigated spherical collapse of a perfect fluid without the assumption of self-similarity [17]. A spherical cloud of counterrotating particles was investigated by the present authors [18]. The spherical gravitational collapse of an imperfect fluid which has only a tangential pressure has also been considered [19–23]. Further, the naked singularity produced by the gravitational collapse of radiation shells [24] and of more general matter [25] were investigated. As for the non-spherically symmetric collapse case, Joshi and Krolak revealed that a naked singularity appears also in the Szekeres spacetime with irrotational dust matter [26]. The global visibility of this singularity was recently analyzed [27].

In this paper we investigate whether a naked singularity, if such exists, is a strong source of gravitational radiation, and we attempt to understand the dynamics and observational meaning of the naked singularity formation. As noted above, several researchers have shown that the final fate of gravitational collapse is not always a singularity covered by an event horizon. In this case with a small disturbance of spacetime, very short wavelength gravitational waves, which are created in the high density region around a singularity, may propagate to the observer outside the dust cloud because of the absence of an event horizon. If this is true, extremely high energy phenomena which cannot be realized in any high energy experiment on Earth can be observed. Moreover, information regarding the physics of so-called ‘quantum gravity’ may be obtained. Also, these waves may be so intense that they destroy the Cauchy horizon. In this paper we consider the generation of gravitational waves during the collapse of a spherical dust ball with a small disturbance of the density profile, i.e. perturbations of LTB spacetime.

Nakamura, Shibata and Nakao [28] have suggested that a naked singularity may emit considerable gravitational wave radiation. This was proposed using an estimate of gravitational radiation from a spindle-like naked singularity. They modeled the spindle-like naked singularity formation in gravitational collapse using a sequence of general relativistic, momentarily static initial data for a prolate spheroid. It should be noted that the system they considered is different from that considered in this article and that their result is controversial. There are numerical analyses that may support or may not support the results of Nakamura, Shibata and Nakao for prolate collapse [13] and for cylindrical collapse [29,30].

Due to the non-linear nature of the problem, it is difficult to analytically solve the Einstein equation. Therefore, numerical methods will provide the final tool. However, its singular behavior makes accurate numerical analysis very difficult at some stage. In this article, we investigate even-parity linear gravitational waves from the collapse of an inhomogeneous spherically symmetric dust cloud. Even for the linearized Einstein equation we must perform numerical integration. However, in contrast to the numerical simulation of the full Einstein equation, high precision is guaranteed for the numerical integration of the linearized Einstein equation, even in regions with extremely large spacetime curvature. Furthermore, the linear stability of known examples of naked singularity formation is necessary as a first step to understand the general dynamics near naked singularity formation.

Recently, Iguchi, Nakao and Harada [31] (INH) studied odd-parity metric perturbations around a naked singularity in the LTB spacetime. In INH, it was found that the propagation of odd-parity gravitational waves is not affected by the collapse of a dust cloud before the formation of the event horizon, even if there appears a central naked singularity. The same authors extended their study to consider the generation of gravitational waves from the dust collapse including matter perturbation [32]. They showed that gauge-invariant variables diverge only at the center, and they do not propagate to the outside. For an odd-parity perturbation the evolution of the matter perturbation decouples from the evolution of the metric perturbation, while the even-parity matter perturbation couples to the metric part. Therefore an even mode seems to be more essential. To investigate the generation of gravitational waves in LTB spacetime we should analyze even-parity perturbations. Here we investigate the behavior of the even-parity quadrupole metric and matter perturbations in the marginally bound LTB background. We numerically calculate the time evolutions of the gauge invariant metric variables. We show that some of metric perturbation variables and the Weyl scalar diverge at the Cauchy horizon but that derived the energy flux does not.

This paper is organized as follows: In Sec. II the basic equations are derived; in Sec. III the numerical results are presented; in Sec. IV we discuss the numerical results; and in Sec. V we summarize our results. We adopt geometrized units in which  $c = G = 1$ . The signature of the metric tensor and sign convention for the Riemann tensor follow Ref. [33].

## II. BASIC EQUATIONS

We consider the evolution of even-parity perturbations of the LTB spacetime to linear order. The background LTB spacetime describes the dynamics of an inhomogeneous spherically symmetric dust ball. Using the synchronous comoving coordinate system, the line element of the LTB spacetime can be expressed in the form

$$d\bar{s}^2 = \bar{g}_{\mu\nu} dx^\mu dx^\nu \equiv -dt^2 + A^2(t, r) dr^2 + R^2(t, r) (d\theta^2 + \sin^2 \theta d\phi^2). \quad (2.1)$$

The energy-momentum tensor for the dust fluid is

$$\bar{T}^{\mu\nu} = \bar{\rho}(t, r) \bar{u}^\mu \bar{u}^\nu, \quad (2.2)$$

where  $\bar{\rho}(t, r)$  is the rest mass density and  $\bar{u}^\mu$  is the 4-velocity of the dust fluid. In the synchronous coordinate system, the unit vector field normal to the spacelike hypersurfaces is geodesic, and there is a freedom concerning which timelike geodesic field is adopted as the hypersurface unit normal. Using this freedom, we can always set  $\bar{u}^\mu = \delta_0^\mu$ , since the 4-velocity of the spherically symmetric dust fluid is tangent to an irrotational timelike geodesic field.

Then the Einstein equations and the equation of motion for the dust fluid reduce to the following simple equations:

$$A = \frac{R'}{\sqrt{1 + f(r)}}, \quad (2.3)$$

$$\bar{\rho}(t, r) = \frac{1}{8\pi} \frac{1}{R^2 R'} \frac{dF(r)}{dr}, \quad (2.4)$$

$$\dot{R}^2 - \frac{F(r)}{R} = f(r). \quad (2.5)$$

Here  $f(r)$  and  $F(r)$  are arbitrary functions of the radial coordinate,  $r$ , and the overdot and prime denote partial derivatives with respect to  $t$  and  $r$ , respectively. From Eq. (2.4),  $F(r)$  is related to the Misner-Sharp mass function [34],  $m(r)$ , of the dust cloud in the manner

$$m(r) = 4\pi \int_0^{R(t,r)} \bar{\rho}(t, r) R^2 dR = 4\pi \int_0^r \bar{\rho}(t, r) R^2 R' dr = \frac{F(r)}{2}. \quad (2.6)$$

Hence Eq. (2.5) might be regarded as the energy equation per unit mass. This means that the other arbitrary function,  $f(r)$ , is recognized as the specific energy of the dust fluid. The motion of the dust cloud is completely specified by the function  $F(r)$  (or equivalently, the initial distribution of the rest mass density,  $\bar{\rho}$ ) and the specific energy,  $f(r)$ . When we restrict our calculation to the case that the symmetric center,  $r = 0$ , is initially regular, the central shell focusing singularity is naked if and only if  $\partial_r^2 \bar{\rho}|_{r=0} < 0$  is initially satisfied for the marginally bound collapse,  $f(r) = 0$  [35,36]. For collapse that is not marginally bound, there exists a similar condition as an inequality for a value depending on the functional forms of  $F(r)$  and  $f(r)$  [10,35,36].

Next we give a brief introduction to the gauge-invariant formalism of Gerlach and Sengupta [37,38] for even-parity perturbations around the most general spherically symmetric spacetime. We consider the general spherically symmetric spacetime with the metric

$$g_{\mu\nu} dx^\mu dx^\nu \equiv g_{ab}(x^d) dx^a dx^b + R^2(x^d) \gamma_{AB}(x^D) dx^A dx^B, \quad (2.7)$$

and stress-energy tensor

$$t_{\mu\nu} dx^\mu dx^\nu \equiv t_{ab}(x^d) dx^a dx^b + \frac{1}{2} t_A^A R^2(x^d) \gamma_{AB}(x^D) dx^A dx^B \quad (2.8)$$

where  $\gamma_{AB} dx^A dx^B = d\theta^2 + \sin^2 \theta d\phi^2$ . Here, lower-case Latin indices refer to radial and time coordinate, while capital Latin indices refer to  $\theta$  and  $\phi$ .

The even-parity perturbations are

$$h_{\mu\nu} = \begin{pmatrix} h_{ab}(x^d) Y & h_a(x^d) Y_{;B} \\ \text{sym} & K(x^d) R^2 \gamma_{AB} Y + G(x^d) R^2 Z_{AB} \end{pmatrix} \quad (2.9)$$

for metric and

$$\delta T_{\mu\nu} = \begin{pmatrix} \Delta t_{ab}(x^d) Y & \Delta t_a(x^d) Y_{;B} \\ \text{sym} & \Delta t^3(x^d) R^2 \gamma_{AB} Y + \Delta t^2(x^d) Z_{AB} \end{pmatrix} \quad (2.10)$$

for matter, where  $Y \equiv Y_l^m(x^D)$  are the scalar spherical harmonics and  $Z_{AB} = Y_{;AB} + \frac{l(l+1)}{2} Y \gamma_{AB}$ . Here covariant derivatives are distinguished as follows:

$$\gamma_{AB;C} \equiv 0, \quad g_{ab|c} \equiv 0. \quad (2.11)$$

For convenience of expression, we introduce

$$v_a \equiv R_{,a}/R \quad (2.12)$$

and

$$p_a \equiv h_a - \frac{1}{2}R^2 G_{,a}. \quad (2.13)$$

A set of even-parity gauge-invariant metric perturbations is defined as

$$k_{ab} \equiv h_{ab} - (p_{a|b} + p_{b|a}) \quad (2.14)$$

$$k \equiv K + \frac{l(l+1)}{2}G - 2v^a p_a. \quad (2.15)$$

A set of even-parity gauge-invariant matter perturbations is defined as

$$T_{ab} \equiv \Delta t_{ab} - t_{ab|c} p^c - t_a^c p_{c|b} - t_b^c p_{c|a}, \quad (2.16)$$

$$T_a \equiv \Delta t_a - t_a^c p_c - R^2(t_A^A/4)G_{,a}, \quad (2.17)$$

$$T^3 \equiv \Delta t^3 - (p^c/R^2)(R^2 t_A^A/2)_{,c} + l(l+1)(t_A^A/4)G, \quad (2.18)$$

$$T^2 \equiv \Delta t^2 - (R^2 t_A^A/2)G. \quad (2.19)$$

The perturbed Einstein equations are expressed only in gauge-invariant perturbations as Eqs. (3.13) of Ref. [38]. We give these equations in Appendix A.

In this paper we restrict our numerical investigation to the quadrupole mode in the marginally bound background. We derive the perturbed equations in that case. Note that, from Eq. (2.3), the background metric variable  $A$  is equal to  $R'$ . Also, we can easily integrate Eq. (2.5) and obtain

$$R(t, r) = \left(\frac{9F}{4}\right)^{1/3} [t_0(r) - t]^{2/3}, \quad (2.20)$$

where  $t_0(r)$  is an arbitrary function of  $r$ . The formation time of the naked singularity is  $t_0 = t_0(0)$ . Using the freedom for the scaling of  $r$ , we choose  $R(0, r) = r$ . This scaling of  $r$  corresponds to the following choice of  $t_0(r)$ :

$$t_0(r) = \frac{2}{3\sqrt{F}} r^{3/2}. \quad (2.21)$$

The energy density  $\bar{\rho}$  is perturbed by adding the scalar term  $\delta\rho Y$ , while the 4-velocity  $\bar{u}_\mu$  is perturbed by adding the term

$$\delta u_\mu = (V_0(x^d)Y, V_1(x^d)Y, V_2(x^d)Y_A). \quad (2.22)$$

The normalization for the 4-velocity yields the relation  $\bar{u}^\mu \delta u_\mu = 0$ . This relation implies that  $V_0$  vanishes exactly. Then there are only three matter perturbation variables,

$$T_{00} = \delta\rho(t, r), \quad (2.23)$$

$$T_{01} = \bar{\rho}V_1(t, r), \quad (2.24)$$

$$T_0 = \bar{\rho}V_2(t, r). \quad (2.25)$$

The others exactly vanish:

$$T_{11} = T_1 = T^3 = T^2 = 0. \quad (2.26)$$

Now we can write down the perturbed Einstein field equations for the background LTB spacetime. The resulting linearized Einstein equations are given in Appendix A.

We have obtained seven differential equations, (A7)–(A13), for seven variables (four metric and three matter). The right-hand sides of four of these equations vanish exactly. Then we can obtain the behavior of the metric variables through the integration of them. We transform these equations into more favorable forms. From Eq. (A4),

$$k_{00} = \frac{1}{R'^2} k_{11}. \quad (2.27)$$

Using this relation and the remaining equations whose r.h.s. vanish, we obtain evolution equations for gauge-invariant metric variables as

$$\begin{aligned}
-\ddot{q} + \frac{1}{R^2}q'' &= \frac{4}{R^2}q + \left(\frac{2}{RR'} + \frac{R''}{R^3}\right)q' + 3\frac{\dot{R}'}{R'}\dot{q} + 4\left(\frac{\dot{R}}{R} - \frac{\dot{R}'}{R'}\right)\dot{k} \\
&+ \frac{2}{R'^3}\left(-\dot{R}'' - \frac{2R'^2\dot{R}}{R^2} - \frac{R''\dot{R}}{R} + \frac{2R'\dot{R}'}{R} + \frac{2R''\dot{R}'}{R'}\right)k_{01} \\
&+ \frac{2}{R'^3}\left(-\dot{R}' + \frac{R'\dot{R}}{R}\right)k_{01}',
\end{aligned} \tag{2.28}$$

$$\ddot{k} = -\frac{2}{R^2}q - \frac{q'}{RR'} + \frac{\dot{R}}{R}\dot{q} - 4\frac{\dot{R}}{R}\dot{k} + \frac{2}{RR'}\left(-\frac{\dot{R}'}{R'} + \frac{\dot{R}}{R}\right)k_{01}, \tag{2.29}$$

$$\dot{k}_{01} = -\frac{\dot{R}'}{R'}k_{01} - q', \tag{2.30}$$

where  $q \equiv k - k_{00}$ . If we solve these three equations for some initial data and for the appropriate boundary conditions, we can follow the full evolution of the metric perturbations. When we substitute these metric perturbations into Eqs. (A7), (A8) and (A10), the matter perturbation variables  $\delta\rho$ ,  $V_1$  and  $V_2$ , respectively, are obtained.

We can also investigate the evolution of the matter perturbations from the linearized conservation equations  $\delta(T^{\mu\nu}_{;\nu}) = 0$ . They reduce to

$$\left(\frac{\delta\rho}{\bar{\rho}}\right)' = \frac{1}{\bar{\rho}R^2R'}\left(\frac{R^2\bar{\rho}}{R'}(k_{01} + V_1)\right)' - \frac{6}{R^2}V_2 - \dot{k} - \frac{3}{2}(\dot{k} - \dot{q}), \tag{2.31}$$

$$\dot{V}_1 = -\frac{1}{2}(k' - q'), \tag{2.32}$$

$$\dot{V}_2 = -\frac{1}{2}(k - q). \tag{2.33}$$

Integration of these equations gives us the time evolution of the matter perturbations. We can check the consistency of the numerical calculation by comparison of these variables and those obtained from Eqs. (A7), (A8) and (A10).

To constrain the boundary conditions in our numerical calculation, we should consider the regularity conditions at the center. These conditions are obtained from requiring that all tensor quantities be expandable in non-negative integer powers of locally Cartesian coordinates near the center [39]. The detailed derivation of these conditions is too complicated to be presented here. We simply quote the results. The regularity conditions for the metric perturbations are

$$k \sim k_0(t)r^2, \quad q \sim q_0(t)r^4, \quad k_{01} \sim k_0(t)r^3. \tag{2.34}$$

For the matter perturbations, the regularity conditions at the center are

$$\delta\rho \sim \delta\rho_0(t)r^2, \quad V_1 \sim V_{10}(t)r, \quad V_2 \sim V_{20}(t)r^2. \tag{2.35}$$

Therefore all the variables we need to calculate vanish at the center.

### III. NUMERICAL METHOD AND RESULTS

We numerically solved the wave equations (2.28)–(2.30). Following the method of previous papers, [31,32] we transformed the wave equation (2.28) into the out-going single-null coordinate system. In this section, we present this coordinate transformation and explain our background and initial data of the perturbations. In the later half of this section, we give our numerical results.

## A. Numerical method

In the previous section it was shown that the perturbation variables  $q, k$  and  $k_{01}$  vanish at the center. A careful treatment of the differential equations may be required near the center for proper propagation through the center. Hence we define the new variables

$$\tilde{q} = qR'^7/R^4, \quad \tilde{k} = kR'^4/R^2, \quad \tilde{k}_{01} = k_{01}R'^5/R^3. \quad (3.1)$$

These new variables are not identically zero at the regular center and do not diverge when they approach the central singularity because of the suppression factor  $R'$ . We rewrite Eqs. (2.28)–(2.30) in terms of these new variables.

Next we perform a coordinate transformation for Eq. (2.28) from the synchronous comoving coordinate system  $(t, r)$  to the single-null coordinate system  $(u, \tilde{r})$ , where  $u$  is the outgoing null coordinate and  $\tilde{r} = r$ . We perform the numerical integration of this equation along two characteristic directions. Therefore we use a double null grid in the numerical calculation. Whereas we integrate Eqs. (2.29) and (2.30) along the direction  $r = \text{const}$ . (Detailed explanations of the single-null coordinate used in our calculation is given in INH.) As a result, we obtain the first order differential equations

$$\frac{1}{\alpha} \frac{d}{du} X = a_1 X + a_2 W + a_3 Z + a_4 \tilde{k} + a_5 \tilde{q}, \quad (3.2)$$

$$\dot{W} = b_1 X + b_2 W + b_3 Z + b_4 \tilde{k} + b_5 \tilde{q}, \quad (3.3)$$

$$\dot{Z} = c_1 X + c_2 W + c_3 Z + c_4 \tilde{k} + c_5 \tilde{q}, \quad (3.4)$$

$$\dot{\tilde{k}} = d_1 X + d_2 W + d_3 Z + d_4 \tilde{k} + d_5 \tilde{q}, \quad (3.5)$$

$$\partial_{\tilde{r}} \tilde{q} = e_1 X + e_2 W + e_3 Z + e_4 \tilde{k} + e_5 \tilde{q}, \quad (3.6)$$

where we have introduced  $X$  and  $W$ , which are defined by Eqs. (3.6) and (3.5), respectively, and

$$Z \equiv \tilde{k}_{01} - \frac{R}{R'} \tilde{q}. \quad (3.7)$$

$\alpha$  is given by

$$\alpha \equiv \frac{1}{\dot{u}}. \quad (3.8)$$

The derivatives in Eqs. (3.2) and (3.6) are given by

$$\frac{d}{du} = \partial_u + \frac{d\tilde{r}}{du} \partial_{\tilde{r}} = \partial_u - \frac{\alpha}{2R'} \partial_{\tilde{r}} = \frac{\alpha}{2} \partial_t - \frac{\alpha}{2R'} \partial_r, \quad (3.9)$$

$$\partial_{\tilde{r}} = -\frac{u'}{\dot{u}} \partial_t + \partial_r = R' \partial_t + \partial_r. \quad (3.10)$$

The coefficients  $a_1, a_2, \dots$  are shown in Appendix B. Equations (3.2) and (3.6) are integrated along the double-null grid. We integrate Eq. (3.2) using the scheme of an explicit first order difference equation, and we use the trapezoidal rule to integrate Eq. (3.6). Equations (3.3)–(3.5) are integrated along the timelike directions  $r = \text{const}$  using a first order difference method. We interpolate variables to estimate the right-hand sides of Eqs. (3.3)–(3.5) at the same radial coordinate  $r$  on the previous out-going null slice.

We adopt the initial rest mass density profile

$$\rho(r) = \rho_0 \frac{1 + \exp\left(-\frac{1}{2} \frac{r_1}{r_2}\right)}{1 + \exp\left(\frac{r^n - r_1^n}{2r_1^{n-1} r_2}\right)}, \quad (3.11)$$

where  $\rho_0$ ,  $r_1$  and  $r_2$  are positive constants, and  $n$  is a positive even integer. As a result the dust fluid spreads all over the space. However, if  $r \gg r_1, r_2$ , then  $\rho(r)$  decreases exponentially, so that the dust cloud is divided between the dense core region and the envelope, which can be considered as the vacuum region. We define a core radius

$$r_{\text{core}} = r_1 + \frac{r_2}{2}. \quad (3.12)$$

If we set  $n = 2$ , there appears a central naked singularity. This singularity becomes locally or globally naked, depending on the parameters  $\rho_0$ ,  $r_1$  and  $r_2$ . However, if the integer  $n$  is greater than 2, the final state of the dust cloud is a black hole for all parameter values. Then we consider three different density profiles connected with three types of the final state of the dust cloud, globally and locally naked singularities and a black hole. The outgoing null coordinate  $u$  is chosen so that it agrees with the proper time at the symmetric center. Corresponding parameters are given in Table I. Using this density profile, we numerically calculated the total gravitational mass of the dust cloud  $M$ . In our calculation we adopted the total mass  $M$  as the unit of the variables.

We give the numerical results from the initial conditions for the perturbations

$$X = \frac{\partial_{\tilde{r}} \tilde{q} - (e_3 Z + e_5 \tilde{q})}{e_1}, \quad (3.13)$$

$$W = -d_5 \tilde{q}, \quad (3.14)$$

$$Z = 4 \frac{R}{\tilde{R} R'} \tilde{q}, \quad (3.15)$$

$$\tilde{k} = -\frac{(3R'b_1 + b_5 - b_2 d_5) \tilde{q}}{b_4}, \quad (3.16)$$

$$\tilde{q} = \left( 1 + \left( \frac{r}{r_3} \right)^2 \right)^{-\frac{5}{2}} \frac{R^2}{\tilde{R}^2} b_4, \quad (3.17)$$

on the initial null surface. Here  $\dot{\tilde{k}}$  vanishes on this surface and  $\dot{W}$  and  $\dot{Z}$  are diminished near the center. We chose  $r_3 = 0.3r_{\text{core}}$ . The main results of our numerical investigation do not depend on the detailed choice of the initial conditions.

TABLE I. Parameters of initial density profiles and damped oscillation frequencies, where  $M = 1$ .

	final state	$\rho_0$	$r_1$	$r_2$	$n$	damped oscillation frequency
(a)	globally naked	$1 \times 10^{-2}$	0.25	0.5	2	—
(b)	locally naked	$1 \times 10^{-1}$	0.25	0.5	2	$0.36+0.096i$
(c)	black hole	$2 \times 10^{-2}$	2	0.4	4	$0.36+0.093i$

## B. Results

First we observe the behavior of the metric variables  $q, k, k_{01}$  and the Weyl scalar, which corresponds to out-going waves,

$$\Psi_4 \equiv C_{\mu\nu\rho\sigma} n^\mu \bar{m}^\nu n^\rho \bar{m}^\sigma \quad (3.18)$$

$$= -\frac{3}{32} \sqrt{\frac{5}{\pi}} \sin^2 \theta \frac{k_{01} - (k - q) R'}{R^2 R'}, \quad (3.19)$$

where

$$n^\mu = \left( \frac{1}{2}, -\frac{1}{2R'}, 0, 0 \right) \quad (3.20)$$

$$\bar{m}^\nu = \left( 0, 0, \frac{1}{\sqrt{2}R}, -\frac{i}{\sqrt{2}R \sin \theta} \right), \quad (3.21)$$

outside the dust cloud. The results are plotted in Fig. 1. We can see that the metric variables  $q, k_{01}$  and the Weyl scalar  $\Psi_4$  diverge when they approach the Cauchy horizon. The asymptotic power indices of these quantities are about  $\sim 0.88$ . On the other hand the metric quantity  $k$  does not diverge when it approaches the Cauchy horizon. The energy flux is computed by constructing the Landau-Lifshitz pseudotensor. We can calculate the radiated power of gravitational waves from this. The result is given in Appendix C. For the quadrupole mode, the total radiated power becomes

$$P = \frac{3}{8\pi} k^2. \quad (3.22)$$

The radiated power of the gravitational waves is proportional to the square of  $k$ . Therefore the system of spherical dust collapse with linear perturbations cannot be expected as a strong source of gravitational waves.

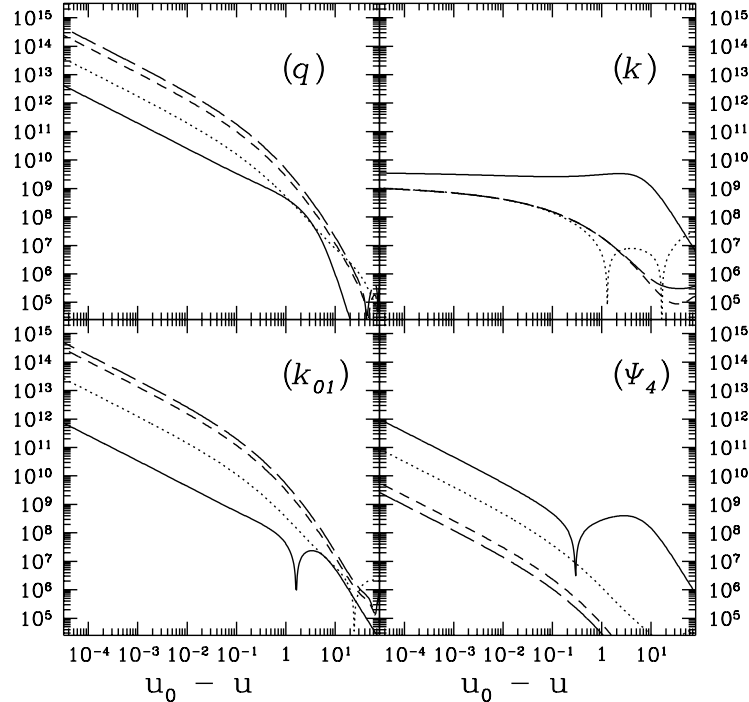


FIG. 1. Plots of perturbed variables  $q, k, k_{01}$  and the Weyl scalar  $\Psi_4$  at constant circumferential radius  $R$ . The results for  $R = 1, R = 10, R = 100$ , and  $R = 200$  are plotted. The solid lines represent the results for  $R = 1$ , the dotted lines for  $R = 10$ , the dashed lines for  $R = 100$ , and the long dashed lines for  $R = 200$ .  $u = u_0$  corresponds to the Cauchy horizon.



Second we observe the perturbations near the center. The results are plotted in Figs. 2 and 3. In these figures we plot the perturbations at  $t - t_0(0) = -10^{-1}, -10^{-2}, -10^{-3}, -10^{-4}$ , and 0. Before the formation of the naked singularity, the perturbations obey the regularity conditions at the center. Each line in these figures displays this dependence if the radial coordinate is sufficiently small. In this region, we can also see that all the variables grow according to power-laws on the time coordinate along the lines of  $r = \text{const}$ . The asymptotic behavior of perturbations near the central naked singularity is summarized as follows:

$$\begin{aligned} q &\propto \Delta t^{-2.1} r^4, & k &\propto \Delta t^{-1.4} r^2, & k_{01} &\propto \Delta t^{-1.0} r^3, \\ \frac{\delta\rho}{\bar{\rho}} &\propto \Delta t^{-1.6} r^2, & V_1 &\propto \Delta t^{-0.4} r, & V_2 &\propto \Delta t^{-0.4} r^2, \end{aligned}$$

where  $\Delta t = t_0(0) - t$ . On the time slice at  $\Delta t = 0$ , perturbations behave as

$$\begin{aligned} q &\propto r^{-0.09}, & k &\propto r^{-0.74}, & k_{01} &\propto r^{0.92}, \\ \frac{\delta\rho}{\bar{\rho}} &\propto r^{-1.4}, & V_1 &\propto r^{0.25}, & V_2 &\propto r^{1.3}. \end{aligned}$$

On this slice  $k$  and  $\delta\rho/\bar{\rho}$  diverge and  $q$  diverges weakly when they approach the central singularity. On the other hand,  $k_{01}$  and  $V_2$  go to zero and  $V_1$  vanishes slowly.

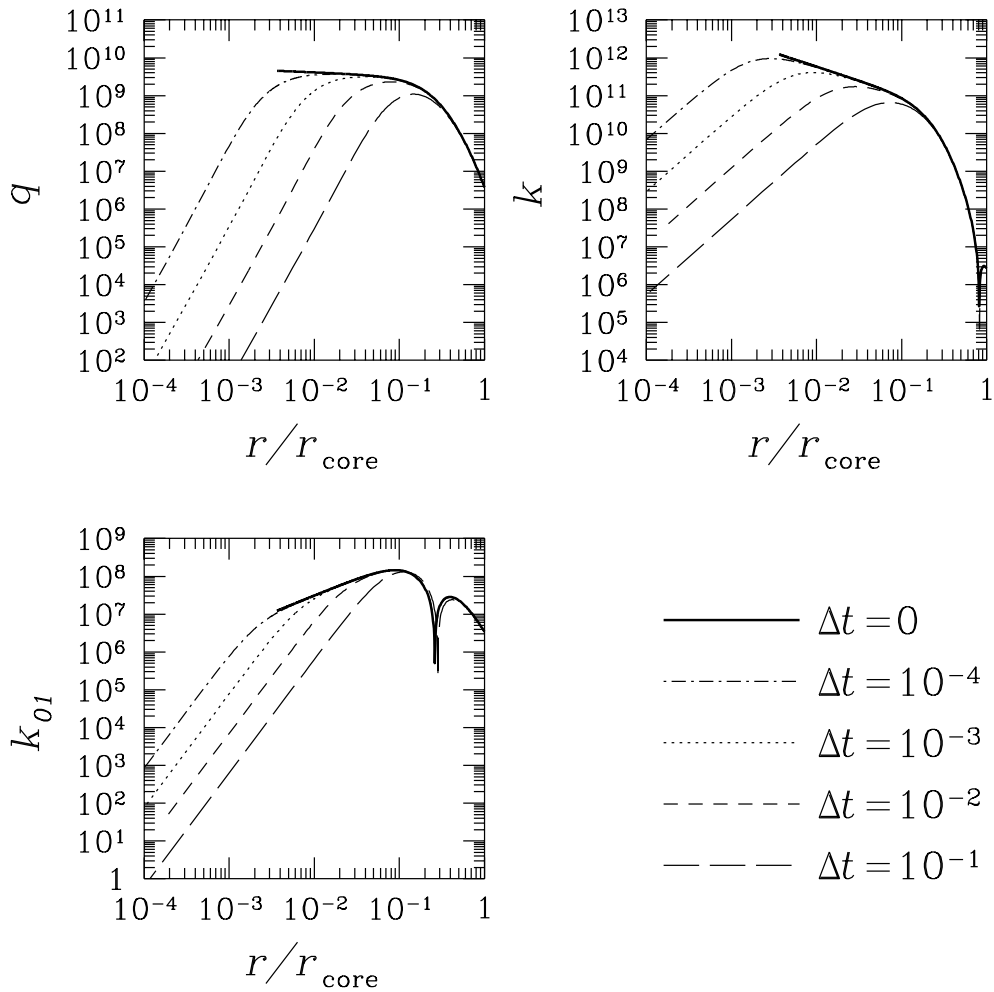


FIG. 2. Plots of perturbed variables  $q$ ,  $k$  and  $k_{01}$  near the center. The values for  $\Delta t = t_0 - t = 10^{-1}, 10^{-2}, 10^{-3}, 10^{-4}, 0$  are plotted. The solid lines represent the results for  $\Delta t = 0$ , the long dashed lines for  $\Delta t = 10^{-1}$ , the dashed lines for  $\Delta t = 10^{-2}$ , the dotted lines for  $\Delta t = 10^{-3}$ , and the dotted dashed lines for  $\Delta t = 10^{-4}$ .

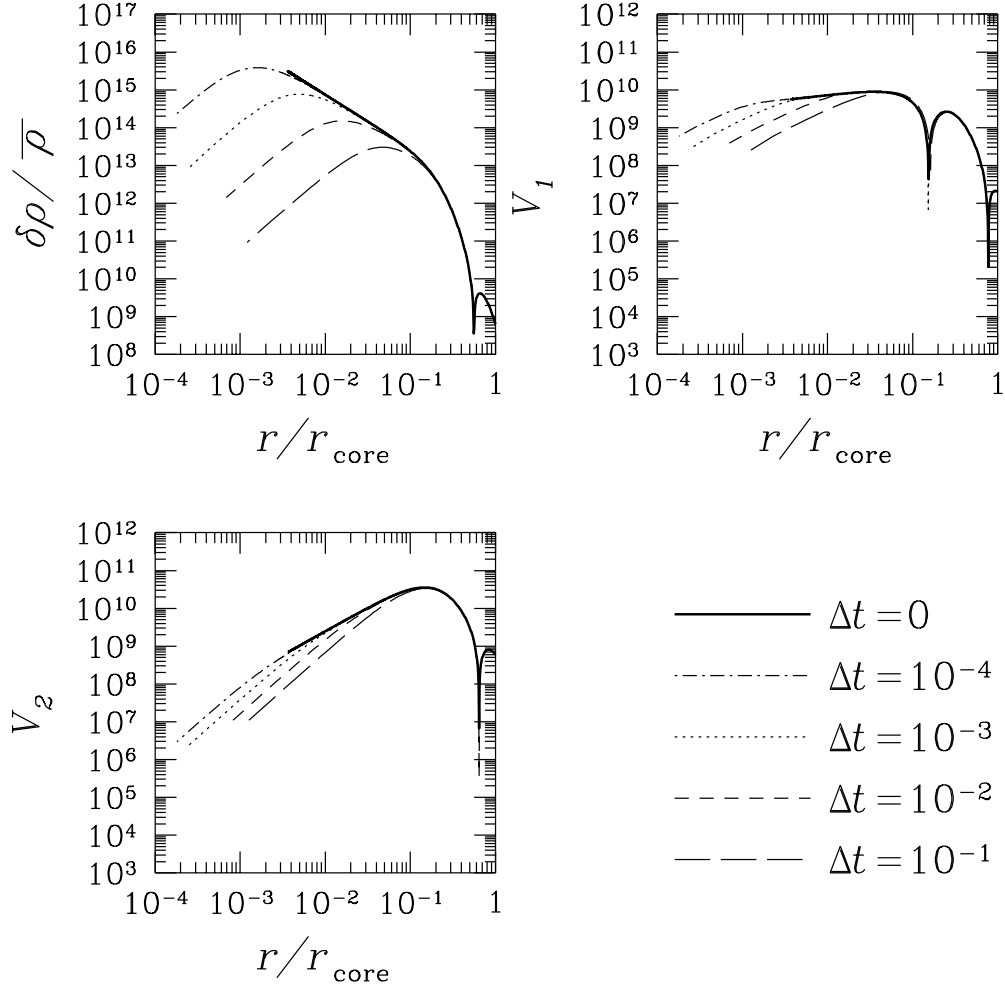


FIG. 3. Plots of perturbed variables  $\delta\rho$ ,  $V_1$ , and  $V_2$  near the center. The values for  $\Delta t = 10^{-1}, 10^{-2}, 10^{-3}, 10^{-4}$ , and 0 are plotted. The solid lines represent the results for  $\Delta t = 0$ , the long dashed lines for  $\Delta t = 10^{-1}$ , the dashed lines for  $\Delta t = 10^{-2}$ , the dotted lines for  $\Delta t = 10^{-3}$ , and the dotted dashed lines for  $\Delta t = 10^{-4}$ .

In cases of a locally naked singularity and black hole formation, we expect to observe damped oscillation in the asymptotic region outside the dust cloud, as in the odd parity case. The results are plotted in Fig. 4. These figures show that damped oscillations are dominant. We read the frequencies and damping rates of these damped oscillations from Fig. 4 and give them in terms of complex frequencies as  $0.36 + 0.096i$  and  $0.36 + 0.093i$  for locally naked and black hole cases, respectively. These results agree well with the fundamental quasi-normal frequency of the quadrupole mode ( $2M\omega = 0.74734 + 0.17792i$ ) [40].

The numerical accuracy of our calculations was checked with the equations that were not used for the derivation of Eqs. (2.28)–(2.30), e.g., Eq. (A10). We define the maximum relative error  $\mathcal{E}$  as

$$\mathcal{E} \equiv \frac{\left| -2\frac{R^3}{R'^8}X + 2\frac{R^2}{R'^4}W + \frac{R^3}{R'^6}\left(6\frac{R''}{R'^2} - \frac{3}{R} - 7\frac{\dot{R}}{R} + 8\frac{\dot{R}'}{R'}\right)Z - \frac{R^3}{R'^7}\partial_{\tilde{r}}Z + \frac{R^2}{R'^4}\left(4\frac{\dot{R}}{R} - 6\frac{\dot{R}'}{R'}\right)\tilde{k} + 16\pi\bar{\rho}V_2 \right|}{\Sigma|\text{each term of numerator}|}. \quad (3.23)$$

We calculated this quantity on the last null surface where the matter variable  $V_2$  is obtained from the integration of Eq. (2.33) using a method similar to that used for Eqs. (3.3)–(3.5). The results are displayed in Fig. 5. Except the region of small  $r$  say, ( $r < 3 \times 10^{-4}$ ), this value is less than 0.01. Both the numerator and denominator of Eq. (3.23) vanish at the center. Therefore it seems difficult to estimate the numerical errors from Eq. (3.23) when  $r$  is small.

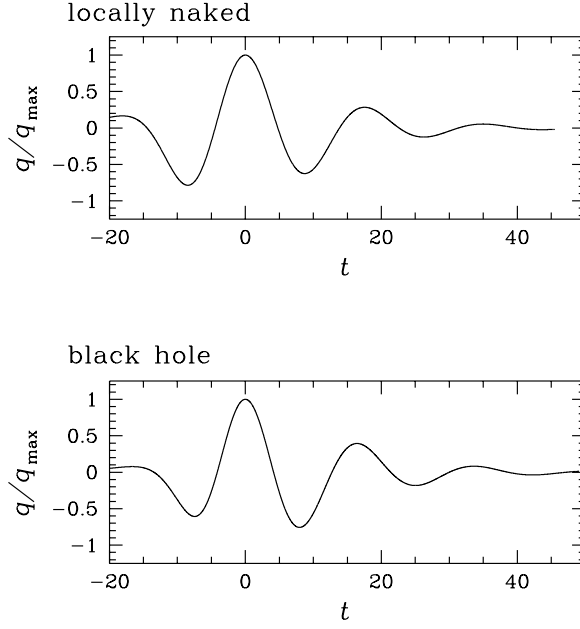


FIG. 4. Plots of perturbed variables  $q$  at constant circumferential radius  $R = 100$  in the locally naked and black hole cases.  $q$  is normalized with respect to its maximum value, and the origin of the time variable is adjusted to coincide with the time when  $q$  is maximum.

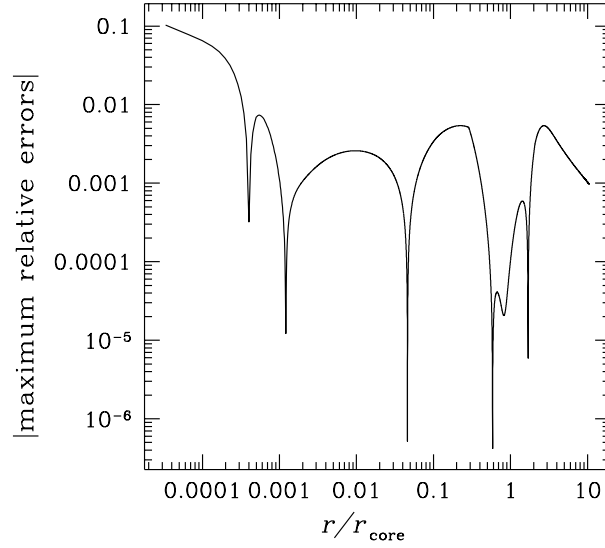


FIG. 5. Maximum relative errors on the last null slice.

#### IV. DISCUSSIONS

In this section we consider the physical interpretation of our numerical results for even-parity perturbations. The divergence behavior of the perturbations implies that the linear perturbation analysis near the Cauchy is invalid. This fact shows that aspherical effects are important in the naked singularity formation.

To consider where these effects are important and what would happen in this region, we should discuss our results more carefully. The perturbations grow according to power-laws and diverge only at the Cauchy horizon. Therefore, except for the region very near the Cauchy horizon, the perturbations are finite and small when we choose sufficiently small initial values. This means that the central region can reach an extremely high density before the breakdown of the linear perturbation analysis. While in the region of spacetime just before the Cauchy horizon, aspherical property becomes important for the dynamics of the spacetime. Our results suggest that the Cauchy horizon is unstable and that a singularity appears along it.

The naked singularity of the LTB spacetime is considered as a massless singularity. Gravitational waves, even if they have finite energy, would affect the naked singularity. To investigate this effect we should consider back-reaction of the gravitational waves.

For the case of collapse that is not marginally bound, the condition of the appearance of the central naked singularity is slightly different from that in the above case [35,36], and hence there is a possibility that the behavior of perturbations in this case is different from that in the marginally bound case. However, it is well known that the limiting behavior of the metric with  $t \rightarrow t_0(r)$  is common to all cases [41]:

$$R \approx \left(\frac{9F}{4}\right)^{1/3} (t_0 - t)^{2/3}, \quad A \approx \left(\frac{2F}{3}\right)^{1/3} \frac{t'_0}{\sqrt{1+f}} (t_0 - t)^{-1/3}. \quad (4.1)$$

Thus we can conjecture that the results of the perturbation analysis for non-marginal collapse would be similar to the results for the marginally bound case.

## V. SUMMARY

We have studied the behavior of even-parity perturbations in the LTB spacetime. We have numerically solved the linearized Einstein equations for gauge-invariant variables in the case of the quadrupole mode and marginally bound background. We have constructed a numerical code which solves the perturbation equations on an out-going single null coordinate. For the globally naked case, the perturbed variables  $q, k_{01}$  and the Weyl scalar  $\Psi_4$  grow as powers of  $(u_0 - u)$  outside the dust cloud, where the power index is approximately  $-0.88$ . Then the Cauchy horizon of this spacetime is unstable with respect to linear even-parity perturbations. On the other hand, the perturbed variable  $k$  is finite just before the crossing of the Cauchy horizon. The energy flux, which is proportional to the square of  $k$ , is also finite. Therefore inhomogeneous aspherical dust collapse is not expected to be a strong source of gravitational wave bursts.

We have investigated the asymptotic behavior of perturbations near a central naked singularity. If the radial coordinate is sufficiently small, the dependence on it is determined by the regularity conditions at the center. Our numerical results show this dependence. The time dependence is an inverse power-law in  $\Delta t$ . At the time of naked singularity formation,  $q, k$  and  $\delta\rho/\bar{\rho}$  diverge when they approach the central singularity, while  $k_{01}, V_1$  and  $V_2$  do not.

For the cases of locally naked and black hole formation, there appear the damped oscillations outside the dust cloud. This is consistent with the fundamental quasi-normal frequency of the quadrupole mode of a Schwarzschild black hole.

## ACKNOWLEDGEMENTS

We would like to thank T. Nakamura for helpful and useful discussions. We are also grateful to H. Sato and colleagues in the theoretical astrophysics group at Kyoto University for useful comments and encouragement. This work was partly supported by Grants-in-Aid for Scientific Research (No. 9204) and Creative Basic Research (No. 09NP0801) from the Japanese Ministry of Education, Science, Sport, and Culture.

## APPENDIX A: LINEARIZED EINSTEIN EQUATIONS

The linearized Einstein equations for the spherically symmetric background presented by Gerlach and Sengupta are

$$\begin{aligned} & 2v^c (k_{ab|c} - k_{ca|b} - k_{cb|a}) - \left[ \frac{l(l+1)}{R^2} + G_c^c + G_A^A + 2\mathcal{R} \right] k_{ab} \\ & - 2g_{ab}v^c (k_{ed|c} - k_{ce|d} - k_{cd|e}) g^{ed} + g_{ab} (2v^c{}^d + 4v^c v^d - G^{cd}) k_{cd} \end{aligned}$$

$$\begin{aligned}
& +g_{ab} \left[ \frac{l(l+1)}{R^2} + \frac{1}{2} (G_c^c + G_A^A) + \mathcal{R} \right] k_d^d + 2(v_a k_{,b} + v_b k_{,a} + k_{,a|b}) \\
& -g_{ab} \left[ 2k_{,c}^{|c} + 6c^c k_{,c} - \frac{(l-1)(l+2)}{R^2} k \right] = -16\pi T_{ab},
\end{aligned} \tag{A1}$$

$$k_{,a} - k_{ac}^{|c} + k_c^c{}_{|a} - v_a k_c^c = -16\pi T_a, \tag{A2}$$

$$\begin{aligned}
& - \left( k_{,c}^{|c} + 2v^c k_{,c} + G_A^A k \right) + \left[ k_{cd}^{|c|d} + 2v^c k_{cd}^{|d} + 2(v^{c|d} + v^c v^d) k_{cd} \right] \\
& -g_{ab} \left[ k_c^c{}_{|d}^{|d} + v^c k_d^d{}_{|c} + \mathcal{R} k_c^c - \frac{l(l+1)}{R^2} k \right] = -16\pi T^3,
\end{aligned} \tag{A3}$$

$$k_c^c = -16\pi T^2, \tag{A4}$$

where  $\mathcal{R}$  is the Gaussian curvature of the 2-dimensional submanifold  $M^2$  spanned by  $x^a$ . Here

$$G_{ab} \equiv -2(v_a|_b + v_a v_b) + g_{ab} \left( 2v_a^{|a} + 3v_a v^a - \frac{1}{R^2} \right), \tag{A5}$$

$$G_A^A \equiv 2(v_a^{|a} + v_a v^a - \mathcal{R}). \tag{A6}$$

For marginally bound LTB spacetime the linearized quadrupole Einstein equations are

$$\begin{aligned}
& \frac{4}{R^2} q + \frac{1}{RR'} q' + \frac{\dot{R}}{R} \dot{q} \\
& - \frac{6}{R^2} k + \left( \frac{2}{RR'} - \frac{R''}{R'^3} \right) k' - \left( 2\frac{\dot{R}}{R} + \frac{\dot{R}'}{R'} \right) \dot{k} + \frac{1}{R'^2} k'' \\
& + 2 \left( \frac{\dot{R}}{R^2 R'} - \frac{\dot{R} R''}{RR'^3} + \frac{\dot{R}'}{RR'^2} \right) k_{01} + 2\frac{\dot{R}}{RR'^2} k_{01}' = -8\pi \delta \rho,
\end{aligned} \tag{A7}$$

$$- \frac{\dot{R}}{R} q' + \frac{R'}{R} \dot{q} + \left( 2\frac{\dot{R}}{R} - \frac{\dot{R}'}{R'} \right) k' + \dot{k}' - \frac{3}{R^2} k_{01} = -8\pi \bar{\rho} V_1, \tag{A8}$$

$$\begin{aligned}
& 2\frac{R'^2}{R^2} q - \frac{R'}{R} q' - \frac{R'^2 \dot{R}}{R} \dot{q} + 4\frac{R'^2 \dot{R}}{R} \dot{k} + R'^2 \ddot{k} \\
& - 2\frac{R' \dot{R}}{R^2} k_{01} - 2\frac{R'}{R} \dot{k}_{01} = 0,
\end{aligned} \tag{A9}$$

$$- 2\frac{\dot{R}'}{R} q - \dot{q} + 2\frac{\dot{R}'}{R'} k + 2\dot{k} + \frac{R''}{R'^3} k_{01} - \frac{1}{R'^2} k_{01}' = -16\pi \bar{\rho} V_2, \tag{A10}$$

$$q' + \dot{k}_{01} + \frac{\dot{R}'}{R'} k_{01} = 0, \tag{A11}$$

$$\begin{aligned}
& \left( \frac{R^2 R''}{R'^3} - 2\frac{R}{R'} \right) q' - \left( 2R\dot{R} + 3\frac{R^2 \dot{R}'}{R'} \right) \dot{q} - \frac{R^2}{R'^2} q'' - R^2 \ddot{q} \\
& + 4 \left( R\dot{R} + \frac{R^2 \dot{R}'}{R'} \right) \dot{k} + 2R^2 \ddot{k} + 2 \left( \frac{RR'' \dot{R}}{R'^3} - \frac{R \dot{R}'}{R'^2} \right) k_{01} \\
& - 2\frac{R \dot{R}}{R'^2} k_{01}' + 2 \left( \frac{R^2 R''}{R'^3} - \frac{R}{R'} \right) \dot{k}_{01} - 2\frac{R^2}{R'^2} \dot{k}_{01}' = 0,
\end{aligned} \tag{A12}$$

$$-k_{00} + \frac{1}{R'^2} k_{11} = 0. \tag{A13}$$

Here we have used Eq. (A13) to eliminate  $k_{11}$  in Eqs. (A7)–(A12).

## APPENDIX B: COEFFICIENTS OF DIFFERENTIAL EQUATIONS

The coefficients of Eqs. (3.2)–(3.6) are

$$a_1 = \frac{1}{R} - \frac{\dot{R}}{R} - 4\frac{R''}{R'^2} + \frac{5}{2}\frac{\dot{R}'}{R'}, \quad (\text{B1})$$

$$a_2 = 2\frac{R'^3}{R^2} \left( R\dot{R}' - R'\dot{R} \right), \quad (\text{B2})$$

$$a_3 = 3\frac{R'^2\dot{R}^2}{R^2} - 3\frac{R'\dot{R}\dot{R}'}{R}, \quad (\text{B3})$$

$$a_4 = -4\frac{R'^4\dot{R}^2}{R^3} + 12\frac{R'^3\dot{R}\dot{R}'}{R^2} - 8\frac{R'^2\dot{R}'^2}{R}, \quad (\text{B4})$$

$$a_5 = -3\frac{R'}{R} - \frac{1}{4}\frac{R'\dot{R}^2}{R} + \frac{1}{2}\dot{R}\dot{R}', \quad (\text{B5})$$

$$b_1 = -\frac{1}{R'^4}, \quad (\text{B6})$$

$$b_2 = -8\frac{\dot{R}}{R} + 8\frac{\dot{R}'}{R'}, \quad (\text{B7})$$

$$b_3 = 0, \quad (\text{B8})$$

$$b_4 = -7\frac{\dot{R}^2}{R^2} + 28\frac{\dot{R}\dot{R}'}{RR'} - 20\frac{\dot{R}'^2}{R'^2}, \quad (\text{B9})$$

$$b_5 = -\frac{3}{R'^3} - 4\frac{\dot{R}}{R'^3} - \frac{9}{2}\frac{\dot{R}^2}{R'^3} + 4\frac{R\dot{R}'}{R'^4} + 4\frac{R\dot{R}\dot{R}'}{R'^4}, \quad (\text{B10})$$

$$c_1 = -\frac{1}{R'^2}, \quad (\text{B11})$$

$$c_2 = 0, \quad (\text{B12})$$

$$c_3 = -5\frac{\dot{R}}{R} + 6\frac{\dot{R}'}{R'}, \quad (\text{B13})$$

$$c_4 = 0, \quad (\text{B14})$$

$$c_5 = -\frac{1 + \dot{R}}{R'}, \quad (\text{B15})$$

$$d_1 = 0, \quad (\text{B16})$$

$$d_2 = 1, \quad (\text{B17})$$

$$d_3 = 0, \quad (\text{B18})$$

$$d_4 = 0, \quad (\text{B19})$$

$$d_5 = \frac{R(1 + \dot{R})}{R'^3}, \quad (\text{B20})$$

$$e_1 = \frac{1}{R}, \quad (\text{B21})$$

$$e_2 = 0, \quad (\text{B22})$$

$$e_3 = 2\frac{R'}{R^2} \left( R'\dot{R} - R\dot{R}' \right), \quad (\text{B23})$$

$$e_4 = 0, \quad (\text{B24})$$

$$e_5 = 7\frac{R''}{R'} - 3\frac{R'}{R} \left( 1 + \dot{R} \right) + 5\dot{R}'. \quad (\text{B25})$$

## APPENDIX C: POWER OF GRAVITATIONAL RADIATION

In this appendix we calculate the radiated power of the gravitational waves in an attempt to grasp the physical meaning of the gauge-invariant quantities [42]. To relate the perturbation of the metric to the radiated gravitational

power, it is useful to specialize to the radiation gauge, in which the tetrad components  $h_{(\theta)(\theta)} - h_{(\phi)(\phi)}$  and  $h_{(\theta)(\phi)}$  fall off as  $O(1/R)$ , and all other tetrad components fall off as  $O(1/R^2)$  or faster. Note that in vacuum at large distance, the spherically symmetric background metric is identical to the Schwarzschild solution, where hereafter we adopt the Schwarzschild coordinates,

$$ds^2 = - \left(1 - \frac{2M}{R}\right) d\tau^2 + \left(1 - \frac{2M}{R}\right)^{-1} dR^2 + R^2 (d\theta^2 + \sin^2 \theta d\phi^2). \quad (\text{C1})$$

The relation between the line elements Eq. (2.1) and Eq. (C1) is given by the transfer matrix

$$d\tau = \frac{1}{1 - (\partial_t R)_r^2} \{dt + (\partial_r R)_t (\partial_t R)_r dr\}, \quad (\text{C2})$$

$$dR = (\partial_t R)_r dt + (\partial_r R)_t dr. \quad (\text{C3})$$

In this gauge, the metric perturbations in Eq. (2.9) behave as

$$h_{ab} = O\left(\frac{1}{R^2}\right), \quad (\text{C4})$$

$$h_a = O\left(\frac{1}{R}\right), \quad (\text{C5})$$

$$K = O\left(\frac{1}{R^2}\right), \quad (\text{C6})$$

$$G = \frac{g(\tau - R_*)}{R} + O\left(\frac{1}{R^2}\right), \quad (\text{C7})$$

where

$$R_* = R + 2M \ln \left( \frac{R}{2M} - 1 \right) + \text{const}, \quad (\text{C8})$$

and the out-going wave condition is respected. Then, the gauge-invariant metric perturbations (2.14) and (2.15) are calculated as

$$k_{\tau\tau} = g^{(2)} R + O(1), \quad (\text{C9})$$

$$k_{\tau R} = -g^{(2)} R + O(1), \quad (\text{C10})$$

$$k_{RR} = g^{(2)} R + O(1), \quad (\text{C11})$$

$$k = -g^{(1)} + O\left(\frac{1}{R}\right), \quad (\text{C12})$$

where  $g^{(1)}$  denotes the first derivative of  $g$  with respect to its argument.

In this radiation gauge, the radiated power  $P$  per unit solid angle is given by the formula derived by Landau and Lifshitz [41] from their stress-energy pseudo-tensor,

$$\frac{dP}{d\Omega} = \frac{R^2}{16\pi} \left[ \left( \frac{\partial h_{(\theta)(\phi)}}{\partial \tau} \right)^2 + \frac{1}{4} \left( \frac{\partial h_{(\theta)(\theta)}}{\partial \tau} - \frac{\partial h_{(\phi)(\phi)}}{\partial \tau} \right)^2 \right]. \quad (\text{C13})$$

For the axisymmetric mode, i.e.  $m = 0$ , the above formula is reduced to

$$\frac{dP}{d\Omega} = \frac{1}{64\pi} (g^{(1)})^2 A_l(\theta), \quad (\text{C14})$$

where

$$A_l(\theta) \equiv \frac{2l+1}{4\pi} \sin^4 \theta \left( \frac{d^2 P_l(\cos \theta)}{(d \cos \theta)^2} \right)^2. \quad (\text{C15})$$

By using the gauge-invariant quantities and integrating over all solid angles, the formula for the power of the gravitational radiation is obtained in the following form:

$$\frac{dP}{d\Omega} = \frac{1}{64\pi} k^2 A_l(\theta), \quad (\text{C16})$$

$$P = \frac{1}{64\pi} B_l k^2, \quad (\text{C17})$$

where

$$B_l \equiv \frac{(l+2)!}{(l-2)!}. \quad (\text{C18})$$

- 
- [1] R. Penrose, Phys. Rev. Lett. **14** (1965) 57.
  - [2] S. W. Hawking, Proc. R. Soc. London **A300** (1967), 187.
  - [3] S. W. Hawking and R. Penrose, Proc. R. Soc. London **A314** (1970), 529.
  - [4] R. Penrose, Riv. Nuovo Cim. **1** (1969), 252.
  - [5] R. Penrose, in *General Relativity, an Einstein Centenary Survey*, ed. S. W. Hawking and W. Israel (Cambridge University Press, 1979), p. 581.
  - [6] R. C. Tolman, Proc. Natl. Acad. Sci. U.S.A. **20** (1934), 169.
  - [7] H. Bondi, Mon. Not. R. Astron. Soc. **107** (1947), 410.
  - [8] D. M. Eardley and L. Smarr, Phys. Rev. **D19** (1979), 2239.
  - [9] D. Christodoulou, Commun. Math. Phys. **93** (1984), 171.
  - [10] R. P. C. A. Newman, Class. Quantum Grav. **3** (1986), 527.
  - [11] P. S. Joshi and I. H. Dwivedi, Phys. Rev. **D47** (1993), 5357.
  - [12] S. Jhingan and P. S. Joshi, Annals of Israel Physical Society Vol. 13 (1997), 357.
  - [13] S. L. Shapiro and S. A. Teukolsky, Phys. Rev. Lett. **66** (1991), 994; Phys. Rev. **D45** (1992), 2006.
  - [14] A. Ori and T. Piran, Phys. Rev. Lett. **59** (1987), 2137.
  - [15] A. Ori and T. Piran, Phys. Rev. **D42** (1990), 1068.
  - [16] P. S. Joshi and I. H. Dwivedi, Commun. Math. Phys. **146** (1992), 333.
  - [17] T. Harada, Phys. Rev. **D58** (1998), 104015.
  - [18] T. Harada, H. Iguchi and K. Nakao, Phys. Rev. **D58** (1998), 041502.
  - [19] G. Magli, Class. Quantum Grav. **14** (1997), 1937.
  - [20] G. Magli, Class. Quantum Grav. **15** (1998), 3215.
  - [21] T. P. Singh and L. Witten, Class. Quant. Grav. **14** (1997), 3489.
  - [22] S. Barve, T. P. Singh and L. Witten, gr-qc/9901080.
  - [23] T. Harada, K. Nakao and H. Iguchi, Class. Quant. Grav. **16** (1999), 2785.
  - [24] I. H. Dwivedi and P. S. Joshi, Class. Quantum Grav. **6** (1989), 1599; **8**, (1991) 1339.
  - [25] I. H. Dwivedi and P. S. Joshi, Commun. Math. Phys. **166** (1994), 117.
  - [26] P. S. Joshi and A. Krolak, Class. Quant. Grav. **13** (1996), 3069.
  - [27] S. S. Deshingkar, S. Jhingan and P. S. Joshi, Gen. Relat. Gravit. **30** (1998), 1477.
  - [28] T. Nakamura, M. Shibata and K. Nakao, Prog. Theor. Phys. **89** (1993), 821.
  - [29] F. Echeverria, Phys. Rev. **D47** (1993), 2271.
  - [30] T. Chiba, Prog. Theor. Phys. **95** (1996), 321.
  - [31] H. Iguchi, K. Nakao and T. Harada, Phys. Rev. **D57** (1998), 7262.
  - [32] H. Iguchi, T. Harada and K. Nakao, Prog. Theor. Phys. **101** (1999), 1235.
  - [33] C. W. Misner, K. S. Thorne and J. A. Wheeler, *Gravitation* (Freeman, San Francisco, 1973).
  - [34] C. W. Misner and D. H. Sharp, Phys. Rev. **136** (1964), B571.
  - [35] T. P. Singh and P. S. Joshi, Class. Quant. Grav. **13** (1996), 559.
  - [36] S. Jhingan, P. S. Joshi and T. P. Singh, Class. Quant. Grav. **13** (1996), 3057.
  - [37] U. H. Gerlach and U. K. Sengupta, Phys. Rev. **D19** (1979), 2268.
  - [38] U. H. Gerlach and U. K. Sengupta, Phys. Rev. **D22** (1980), 1300.
  - [39] J. M. Bardeen and T. Piran, Phys. Rep. **96** (1983), 205.
  - [40] S. Chandrasekhar and S. Detweiler, Proc. R. Soc. London, **344** (1975), 441.
  - [41] L. D. Landau and E. M. Lifshitz, *The Classical Theory of Fields* (Pergamon, London, 1975).
  - [42] C. T. Cunningham, R. H. Price, and V. Moncrief, Astrophys. J. **224** (1978), 643; **230** (1978), 870; **236** (1980), 674.